JOURNAL OF THE MECHANICAL BEHAVIOR OF BIOMEDICAL MATERIALS 46 (2015) 41–48

Available online at www.sciencedirect.com

ScienceDirect

www.elsevier.com/locate/jmbbm

Research Paper

Creep-assisted slow crack growth in bio-inspired dental multilayers

Jing Du[a,b], *Xinrui Niu*[c], *Wole Soboyejo*[a,b,*]

[a]*Department of Mechanical and Aerospace Engineering, Princeton University, Princeton, NJ 08544, USA*
[b]*The Princeton Institute for the Science and Technology of Materials (PRISM), Princeton University, Princeton, NJ 08544, USA*
[c]*Department of Mechanical and Biomedical Engineering, City University of Hong Kong, Kowloon, Hong Kong, China*

ARTICLE INFO

Article history:
Received 10 October 2014
Received in revised form
22 January 2015
Accepted 26 January 2015
Available online 3 February 2015

Keywords:
Creep
Slow crack growth
Hertzian contact
Dental multilayers

ABSTRACT

Ceramic crown structures under occlusal contact are often idealized as flat multilayered structures that are deformed under Hertzian contact loading. Previous models treated each layer as linear elastic materials and resulted in differences between the measured and predicted critical loads. This paper examines the combined effects of creep (in the adhesive and substrate layers) and creep-assisted slow crack growth (in the ceramic layer) on the contact-induced deformation of bio-inspired, functionally graded multilayer (FGM) structures and the conventional tri-layers. The time-dependent moduli of each of the layers were determined from constant load creep tests. The resulting modulus–time characteristics were modeled using Prony series. These were then incorporated into a finite element model for the computation of stress distributions in the sub-surface regions of the top ceramic layer, in which sub-surface radial cracks, are observed as the clinical failure mode. The time-dependent stresses are incorporated into a slow crack growth (SCG) model that is used to predict the critical loads of the dental multilayers under Hertzian contact loading. The predicted loading rate dependence of the critical loads is shown to be consistent with experimental results. The implications of the results are then discussed for the design of robust dental multilayers.

1. Introduction

The study of the contact loading of dental restorations/crowns is often conducted on idealized, flat multilayered structures, that are deformed under Hertzian contact loading (Kelly, 1997; Lawn et al., 2000, 2004; Lee et al., 2002; Malament and Socransky, 1999; Rekow and Thompson, 2007; Zhang et al., 2004). This often leads to the onset of clinically-relevant sub-surface radial cracking, due to the high stress concentrations in the sub-surface regions in the top ceramic layer (Huang et al., 2007b; Shrotriya et al., 2003). Such radial cracking is also consistent with the major clinical failure mode reported by Kelly (1997).*

Abbreviations: DEJ, dento-enamel-junction; FEM, finite element method; FGM, functionally graded multilayer; SCG, slow crack growth; CASCG, creep-assisted slow crack growth

*Corresponding author at: Department of Mechanical & Aerospace Engineering, Engineering Quadrangle Room D404B, Princeton, #NJ 08544, USA. Tel.: +1 609 258 5609; fax: +1 609 258 5877.
E-mail addresses: jingdu@alumni.princeton.edu (J. Du), xinrui.niu@cityu.edu.hk (X. Niu), soboyejo@princeton.edu (W. Soboyejo).

http://dx.doi.org/10.1016/j.jmbbm.2015.01.019
1751-6161/

The opportunity to reduce the stress concentrations at the bottom of the top ceramic layer in dental multilayers was inspired by nanoindentation measurements on the dento-enamel-junction (DEJ) (Marshall et al., 2001). Their studies showed that the Young's modulus varies across the DEJ. Inspired by the gradation in Young's modulus across the DEJ, Huang et al. (2007b) developed a finite element model of the bio-inspired functionally graded multilayer (FGM) of ceramic crown structures. Their results showed that, under Hertzian contact, the FGM structure results in lower stresses in the sub-surface region of the top ceramic layer.

Subsequent work by Niu et al. (2009) and Rahbar and Soboyejo (2011) also showed similar reductions in stress concentrations in the top ceramic crown layer by using FGMs. These were later confirmed by the experimental work by Niu et al. (2009) and Du et al. (2013), who conducted contact loading experiments on actual FGM structures that were fabricated with nanocomposite layers. These had ~20–40% greater critical pop-in loads than flat conventional dental multilayers without FGMs. Also, since the FGM structure has a higher stiffness than the conventional single adhesive layer, it serves as a stress buffer to the top ceramic layer, by dissipating stress from the top ceramic layer into the FGM.

The pop-in loads in the bio-inspired and flat conventional dental multilayers have been predicted using a slow crack growth (SCG) model. This is a power law model that describes the stable crack growth behavior (Wiederhorn, 1974) in the top ceramic layers. It was adopted by researchers (Huang et al., 2007a; Lee et al., 2002; Niu and Soboyejo, 2006; Zhang et al., 2004) to explain subsurface radial crack growth in the top ceramic layers. It was also used to predict the critical pop-in loads in dental multilayers under Hertzian contact loading.

However, although the SCG model predicts the contact damage due to the slow crack growth in the top ceramic layer, it treats the middle adhesive layer and substrate layers as linear elastic materials. Furthermore, there is clear evidence of viscous flow in the substrate and middle layers of dental multilayers (Huang et al., 2007a; Lee et al., 2002; Niu and Soboyejo, 2006; Zhang et al., 2004) that is not accounted for in the conventional dental multilayered structures.

Hence, it has been suggested that the differences between the measured and predicted critical loads (that were obtained from these systems) were due to substrate creep effects (Lee et al., 2002). Furthermore, the differences between critical loads of structures with and without FGM were observed to be greater at slower loading rates than at faster loading rates (Du et al., 2013; Niu et al., 2009). These differences suggest that creep effects should be considered in the modeling of layer properties.

In prior studies, Niu and Soboyejo (2006) modeled the viscoelastic deformation of dental multilayers with rate-dependent elastic moduli. The elastic modulus for specific loading rate was measured from stress–strain data that was obtained from compression tests at particular loading rates. The limitation of this method is that the rate-dependent elastic modulus can only be used in the simulation of the Hertzian contact under the same loading rate. Hence, in order to simulate the Hertzian contact under various loading rates, compression tests have to be performed at each of the loading rates.

In this paper, the viscosity of the each layer in model dental multilayers is measured using creep experiments. The measured viscous behavior is then modeled using Prony series (Bower, 2011). The Prony series fits to the experimental data are compared with those obtained from other models. A creep-assisted slow crack growth model is then developed. The model, which incorporates the combined effects of slow crack growth (in the top ceramic layers) and the viscosity of the adhesive and substrate layers, is used to predict the critical pop-in loads. The implications of the results are then discussed for the design of robust, bio-inspired, dental multilayer structures.

2. Materials and experimental methods

2.1. *Fabrication of bio-inspired FGM dental structures*

The bio-inspired FGM structure was fabricated using a steel plate mold with a thickness of ~4 mm and an inner diameter of ~9 mm. The substrate was a dentin-like soft material, Z100 restorative (3M ESPE Dental Products, St. Paul, MN), which is a clinically-used dental material. It was poured into the mold and then cured with UV light. The FGM was produced using nanocomposite mixtures of zirconia or alumina nanoparticles (Nanotek Instrument Inc., Dayton, OH) and an epoxy matrix, EPO-TEK 301 (Epoxy Technology Inc., Billerica, MA). After mixing, the nanocomposite material was deposited in the steel mold and then cured in a vacuum oven at a temperature of 65 °C. The deposition and curing process were then repeated to build up the multilayers.

The crown-like dental ceramic layer on top was fabricated from a medical grade 3 mol% yttria-stabilized zirconia rod (YTZP, Saint-Gobain, Colorado Springs, CO). It was pressed onto the last layer of the FGM before curing. Finally, the multilayered structures, with a diameter of ~9 mm and a thickness of ~5 mm, were cut and removed from the mold. They were then cleaned with distilled water and blow dried with compressed air.

2.2. *Hertzian contact experiments*

Hertzian contact experiments were performed on the fabricated dental multilayers (Fig. 1a). The tests were carried out in an Instron 8872 hydraulic mechanical tester (Instron, Canton, MA, USA). They were conducted in air at room temperature and a relative humidity of ~25%. The Hertzian contact tests were performed under load control with a hemispherical tungsten carbide indenter with a diameter of 20 mm. The tests conducted at clinically relevant loading rates between 1 N/s and 1000 N/s (Du et al., 2013). The loads and displacements were recorded by the computer attached to the Instron tester. The critical loads were then determined as the loads at which discontinuities in displacement were observed. These were also found to correspond to the onset of cracking, which could be heard clearly during the tests.

2.3. *Creep experiments*

The creep specimens were fabricated using the same steel mold that was described above. The nanocomposite materials for

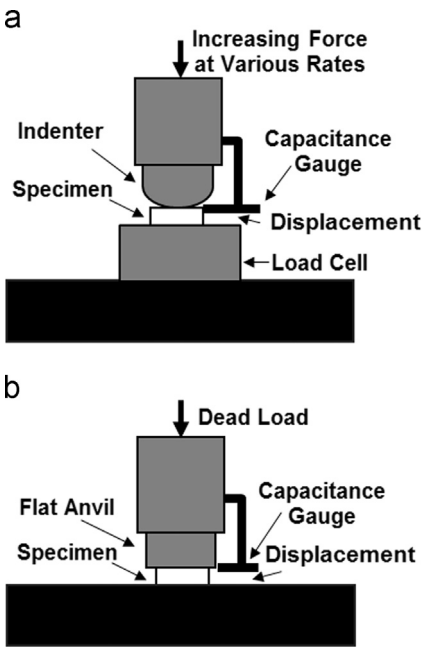

Fig. 1 – Schematics of (a) Hertzian contact test and (b) creep test.

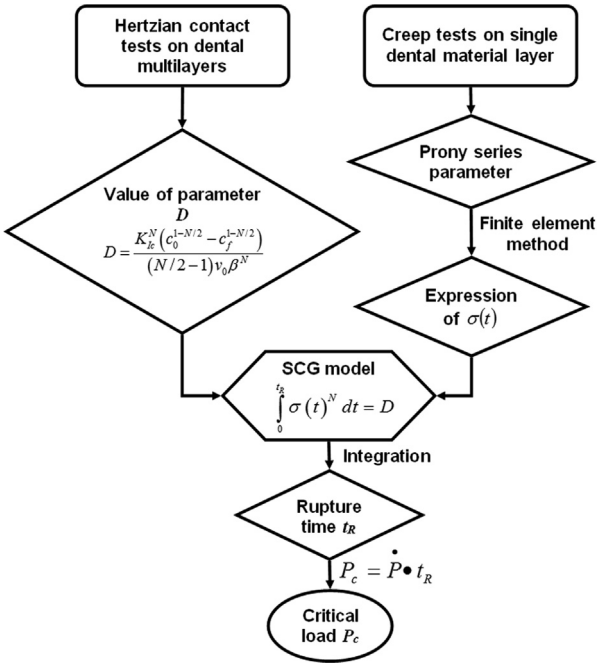

Fig. 2 – Finite element model of dental multilayer structure subjected to Hertzian contact loading.

each FGM layer were filled separately into the steel mold and cured in the vacuum oven at 65 °C. The nanocomposite layers consisted of epoxy matrix and 10 wt% zirconia, 20 wt% zirconia, 30 wt% zirconia, 40 wt% zirconia, 50 wt% zirconia, 60 wt% zirconia, 70 wt% zirconia, 40 wt% alumina and 45 wt% alumina reinforcements. The substrate material, Z100 restorative, was also molded and cured with UV light for 40 s for both sides. The cured materials were then removed from the mold, polished and cleaned with distilled water. Each specimen has a diameter of ~9 mm, a thickness of ~4 mm, and the surface roughness corresponding to 600 grit sand papers.

Creep tests were carried out in a self-built creep tester (Fig. 1b). It was similar to compression test without friction (homogenous compression). A dead load of 139.2 N was applied to the specimen through a flat anvil. The applied compression stress was about 260 MPa. The deformation of the specimen was detected using a capacitance gauge (Capacitec, Ayer, MA). The resulting displacements were recorded using the LABView software package (National Instruments, Austin, TX). Each test lasted for about 24 h. For each material, between 4 and 5 specimens were tested.

3. Modeling

3.1. Constitutive equations

In an effort to develop a viscous model that can be used over a range of loading rates, a three-parameter spring-dashpot solid model (Zener model) has been used to describe the viscous behavior of dental multilayers (Huang et al., 2005, 2007a; Zhou et al., 2007). However, the model, which has only one dashpot, was found to be insufficient for the description of long-term polymer creep behavior (Huang et al., 2007a). There is, therefore, a need for an improved model for the characterization of the viscoelastic behavior of dental multilayered structures.

Since the relaxation times of polymers occur in a distribution, due to the heterogeneity of the polymeric structures (McCrum et al., 1997), Prony series use a series of relaxation times to fully describe the creep or relaxation of polymeric structures, over an extended period of time. Prony series are given by (Bower, 2011)

$$G(t) = G_0\left(1-\sum_{i=1}^{N} g_i\left(1-e^{-t/\tau_i}\right)\right) \quad (1)$$

where $G(t)$ is the time-dependent shear modulus; G_0 is the instantaneous modulus; τ_i is the relaxation time and g_i is the relaxation coefficient. When there is only one exponential term, the Prony series is equivalent to the Zener model.

3.2. Finite element simulations

The finite element simulations were carried out using the Abaqus FEA software package (Dassault Systemes Simulia Corporation, Providence, RI). The stress distributions in the dental multilayers were calculated. Axisymmetric geometries were used to simplify the problem, as shown in Fig. 2. The thickness of the bonding layer was modeled to be 100 μm. A 4-node linear axisymmetric quadrilateral element was used in the mesh. In an effort to capture the high stress concentrations, the mesh was dense in the regions near the axisymmetric axis of the model. The bottom of the substrate was fixed, while the axisymmetric boundary condition was added on the axisymmetric axis.

The simulations considered bio-inspired dental FGM multilayers, as well as structures joined by single adhesive material. The materials and the properties used in the simulation for glass-epoxy-polycarbonate and zirconia-FGM-Z100 multilayer structures are listed in Tables 1 and 2,

respectively. The Prony series parameters were obtained from the creep test experiments. The FGM was modeled as 10 sub layers, with equal layer thicknesses. The elastic moduli for the FGM composites materials were measured using nanoindentation techniques described in detail in a prior study (Du et al., 2013). The Poisson ratio was assumed to be 0.2 for ceramic materials and 0.4 for polymeric and composite materials.

A load of 2500 N was applied to the Hertzian indenter, which was modeled as a rigid surface. In the simulations that consider linear elastic material properties, the load was applied instantaneously. In the contrast, in the simulations that consider the viscous material properties, the load was applied gradually in a linear ramp in durations of 2.5, 25, 250 and 2500 s. They were used, respectively, to simulate loading rates of 1000, 100, 10 and 1 N/s.

3.3. *Creep-assisted slow crack (CASCG) growth model*

The tensile stress at the sub-surface center of the top ceramic layer is associated with the major clinical failure mode, the subsurface radial crack (Kelly, 1997), in the dental multilayer. The slow crack growth (SCG) model suggests that, during contact damage in dental multilayers, sub-surface radial crack growth occurs solely as a result of slow crack growth in the top ceramic layers (Lee et al., 2002; Niu and Soboyejo, 2006; Zhang et al., 2004). For cases in which the initial crack length is very small, and the final crack length is much greater than the initial crack length, the radial crack propagation can be described by the standard power law slow crack growth theory (Dabbs et al., 1982; Lee et al., 2002). This gives

$$\int_0^{t_R} \sigma(t)^N dt = D \tag{2}$$

where t is the time; $\sigma(t)$ is time dependent expression of the tensile stress in the radial direction at subsurface center of the top ceramic layer that will introduce mode I crack into the sub-surface regions of the top ceramic layer; t_R is the rupture time, at which sub-surface radial cracks occur. When the loading rate, $\dot{P}$, is constant, the rupture time, t_R, can be expressed as $t_R = P_c/\dot{P}$, where P_c is the critical "pop-in" load. The parameter, D, in Eq. (2) is a time and load-independent quantity that is given by (Huang et al., 2007a)

$$D = \frac{K_{Ic}^N \left(c_0^{1-N/2} - c_f^{1-N/2}\right)}{(N/2-1)v_0\beta^N} \tag{3}$$

where K_{Ic} is the fracture toughness; N is the crack velocity exponent, which in this case is 25 for zirconia; v_0 is the crack velocity; c_0 and c_f are the initial and final radial crack size; β is a crack geometry coefficient (Dabbs et al., 1982; Huang et al., 2007a; Lee et al., 2002).

The processes involved in the creep-assisted slow crack growth (CASCG) model are illustrated in Fig. 3. By incorporating the actual measurements of Prony series parameters (obtained from the creep test) into the finite element simulations, an expression was obtained for the time-dependent stress, $\sigma(t)$. The critical load versus loading rate obtained from the Hertzian contact experiments was then used to fit the value of D. Since D is only related to material properties and geometry, it should be consistent for different loading rates. Therefore, with D known, Eq. (2) was integrated to obtain the rupture time, t_R, and then the critical load P_c.

Table 1 – Mechanical properties of glass-epoxy-polycarbonate multilayer structure used in the FEM calculation.

Mechanical properties	Material		
	Glass	Epoxy	Polycarbonate
Elastic modulus,E(GPa)	70	3.2	2.3
Poisson's ratio, ν	0.2	0.4	0.4
g_1	–	0.73	0.36
g_2	–	–	0.29
τ_1 (s)	–	54.98	153.8
τ_2(s)	–	–	3790

4. Results and discussion

4.1. *Viscoelastic behavior of single dental layer*

The time-dependent shear moduli measured from creep tests (on the FGM dental structure) are illustrated in Fig. 4. The measured moduli appeared to have discrete values, because the measured deformation values were limited by the spatial resolution of the capacitance gauge that was used in the constant load creep test. Fig. 4a presents a comparison of epoxy nanocomposite materials with 10 wt%, 20 wt%, etc.,

Table 2 – Mechanical properties of zirconia-FGM-Z100 multilayer structure used in the FEM calculation.

Material	Elastic modulusE(GPa)	Poisson's ratio ν	g_1	g_2	g_3	$\sum g_i$	τ_1 (s)	τ_2(s)	τ_3 (s)
Zirconia	205	0.2	–	–	–		–	–	–
Epoxy+10 wt% zirconia	3.33	0.4	0.15	0.19	0.14	0.48	50.42	1542	32,670
Epoxy+20 wt% zirconia	3.82	0.4	0.20	0.17	0.17	0.54	93.85	3002	41,330
Epoxy+30 wt% zirconia	3.95	0.4	0.27	0.13	0.15	0.55	42.19	2489	73,140
Epoxy+40 wt% zirconia	5.10	0.4	0.23	0.15	0.18	0.56	21.17	807	20,510
Epoxy+50 wt% zirconia	7.50	0.4	0.26	0.23	0.15	0.64	12.76	3739	109,200
Epoxy+60 wt% zirconia	7.92	0.4	0.38	0.16	0.10	0.64	181.70	6543	38,970
Epoxy+70 wt% zirconia	9.98	0.4	0.45	0.19	0.15	0.79	1.00	2570	45,710
Epoxy+40 wt% alumina	13.83	0.4	0.58	0.10	0.08	0.76	12.94	3897	65,150
Epoxy+45 wt% alumina	10.30	0.4	0.44	0.14	0.15	0.73	8.68	1330	20,880
Z100	18	0.4	0.59	0.19	0.09	0.87	23.14	748	18,020

and 70 wt% zirconia particles. In general, for composites with the same type of ceramic reinforcements, increased ceramic reinforcement weight fraction resulted in higher instantaneous moduli and relaxed moduli.

The measured shear moduli are presented in Fig. 4b. These are presented for epoxy nanocomposite with 40 wt% and 45 wt% alumina particles, as well as Z100 dental material, which is also a ceramic filled polymeric composite. The instantaneous modulus of Z100 was much greater than that of the alumina filled epoxy composites. However, the relaxed modulus for Z100 was smaller than those of the two epoxy/alumina composites. This indicates greater decay of the modulus of the Z100 samples over time.

The measured creep rates of the epoxy composites with similar weight percentages of zirconia and alumina fillers are compared in Fig. 4c. The alumina-reinforced composites had higher instantaneous moduli than the zirconia-reinforced composites, since alumina has a higher modulus than zirconia. However, these relaxed moduli were similar. This indicates greater modulus decay for the alumina-reinforced epoxy composites.

The time-dependence of shear modulus was modeled using several viscoelastic behavior models. Fig. 5a shows that the Zener model, with a single relaxation time, is not sufficient to capture the creep behavior of polycarbonate over a duration of 15,000 s. However, the predictions from the Prony series model, with two relaxation times, are in closer agreement with the experimental data. Furthermore, the Prony series model also exhibits good agreement with experimental data obtained for polycarbonate and epoxy (Fig. 5b). The resulting Prony series parameters for polycarbonate and epoxy are presented in Table 1.

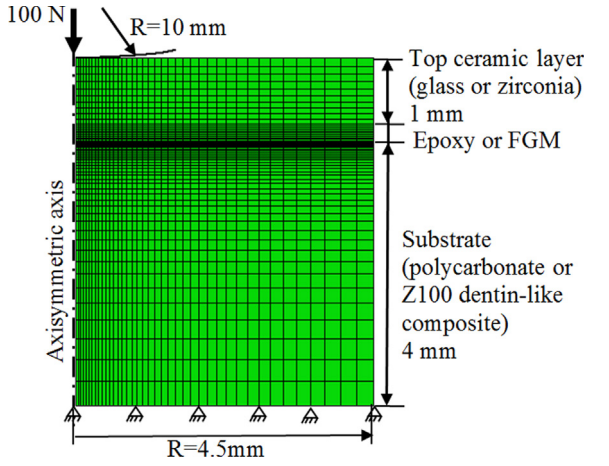

Fig. 3 – Flow chart illustrating process of creep-assisted slow crack growth (CASCG) model.

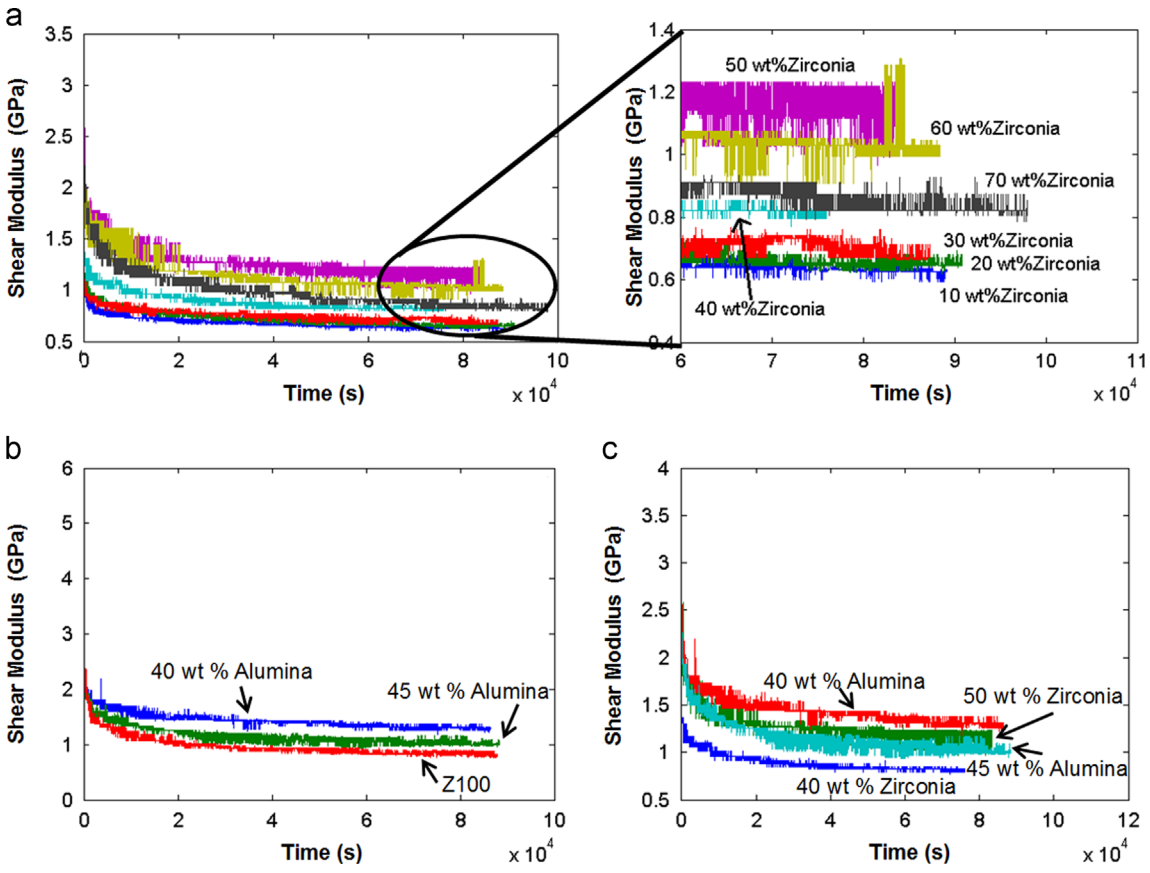

Fig. 4 – Measured shear moduli (as a function of time) obtained for single dental material layers under constant load (in zirconia-FGM-Z100 structure): (a) epoxy reinforced by various weight fractions of zirconia powders, (b) epoxy reinforced with various weight fractions of alumina (Z100 dental composite material included for comparison), and (c) comparison of epoxy reinforced with similar weight fraction of zirconia and alumina powder.

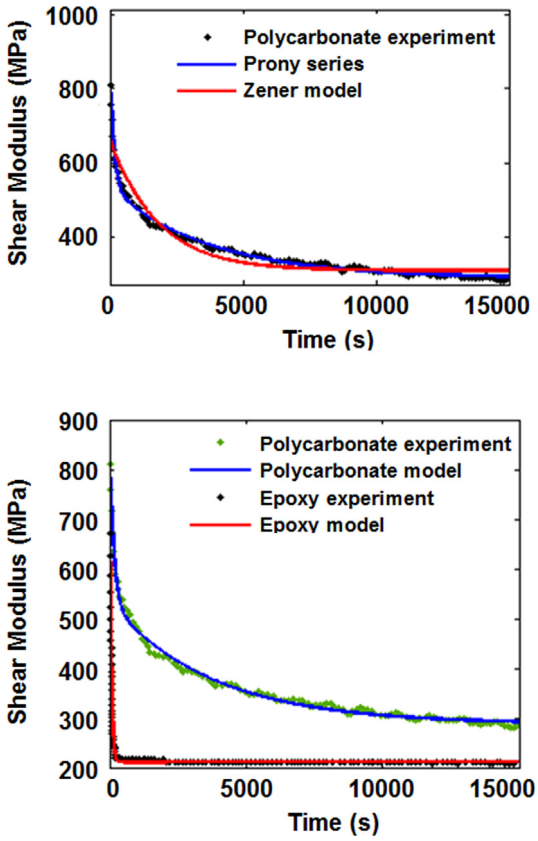

Fig. 5 – Comparison of measured (Huang et al., 2007a) and modeled time dependence of shear modulus in single dental material layers deformed under constant load in a glass-epoxy-polycarbonate structure: (a) comparison of Zener model and Prony series model (for polycarbonate) and (b) Prony series models for epoxy and polycarbonate.

The Prony series predictions obtained for the time-dependence shear modulus are presented in Fig. 6 for a typical single layer in the FGM, containing epoxy reinforced by 70 wt% zirconia. For Prony series with one to three exponential terms, the results show that the range of relaxation time increases with increasing number of exponential terms. Furthermore, the Prony series predictions were in closer agreement with the experimental data, as the number of exponential terms increased. Also, for a duration of ~1 day (10^5 s), three exponential terms were needed to model the creep behavior.

A summary of the Prony series parameters obtained for the FGM layers is presented in Table 2. The coefficients of determination, R^2, of the curve fittings were all greater than 0.85. The experimental results fell in the trend line of Prony series. Each relaxation coefficient $g_i$represents the percentage of modulus decay with the corresponding relaxation time τ_i. Due to the heterogeneity of polymers and the limited resolution of capacitance gauge, the trends of g_i or τ_i were not clear. The summation of the relaxation coefficients, Σg_i, represents the total scale of the modulus decay over time. This increased with increasing zirconia or alumina reinforcement weight fraction. The alumina-reinforced composites had higher Σg_i than the zirconia-reinforced composites. This indicates greater modulus decay of the alumina-reinforced epoxy composites. The Z100 has the highest Σg_i of all the materials

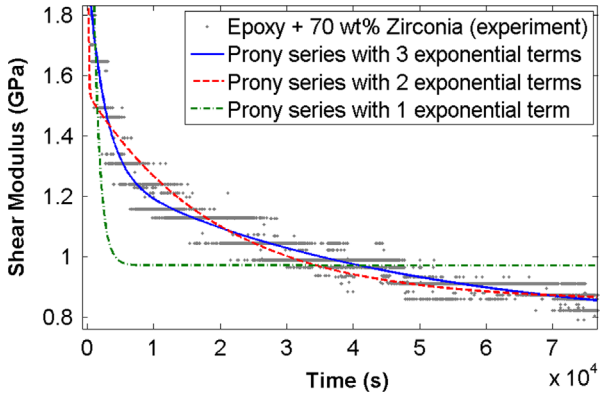

Fig. 6 – Comparison of measured and modeled time dependence of shear modulus obtained for epoxy reinforced with 70 wt% zirconia (a comparison of Prony series with 1, 2 and 3 exponential terms).

presented in Table 2. This is consistent with the trends presented in Fig. 4b and c, in which the Z100 material exhibits the greatest decay of modulus over time.

4.2. *Critical "pop-in" loads of glass-epoxy-polycarbonate tri-layer*

The critical "pop-in" loads obtained for the glass-epoxy-polycarbonate multilayers that were tested under Hertzian contact loading (at various loading rates) are presented in Fig. 7. This includes a comparison of experimental data (Lee et al., 2002) and predictions from different models. In general, the critical "pop-in" loads increased with increasing loading rate. When linear elastic models were used in the FEM simulations, the critical "pop-in" loads predicted from the SCG model (without creep) fall on a straight line in the log-log plot of the critical load vs loading rate shown in Fig. 7. However, the experimental data did not show the same trend. They were generally smaller than the predictions from the linear elastic models at slower loading rates.

When viscoelastic models were used in the FEM simulation, the critical loads predicted by the CASCG model fall on concave curves presented in Fig. 7. At faster loading rates, the slopes of the curves obtained from SCG model (with and without creep) were similar. The slopes of the curves obtained from both Zener model and Prony series increased with decreasing loading rate, because the viscous components in the models have more time to respond and relax at slower loading rates. When the Zener model was used (Huang et al., 2007a), the slopes of the curves did not increase as quickly with decreasing loading rates as those when Prony series were used. The predictions obtained from Prony series were also in closer agreement with the experimental data. The improved agreement with the predictions from the Prony series model is partly attributed to the fact that the Prony series model captures the relaxation of each individual dental layer at various relaxation times (Fig. 5).

4.3. *Critical loads of bio-inspired dental FGM structures*

In the case of the FGM structures, the computed tensile stresses associated with SCG in the subsurface regions of

the top ceramic layer are presented in Fig. 8. The tensile stresses increase with increasing Hertzian contact load. The stresses obtained from the viscoelastic models were greater than those obtained from linear elastic models. The differences between the stresses were greater at slower loading rates, where the viscous components had more time to respond. Furthermore, at slower loading rates, the FGM was less stiff. It, therefore, provided less support to the top ceramic layer than at faster loading rates. Hence, the stresses in the top ceramic layer were higher at slower loading rates. Hence, according to Eq. (2), the stress accumulated more rapidly at slower loading rates. This explains the lower critical loads that we obtained at slower loading rates.

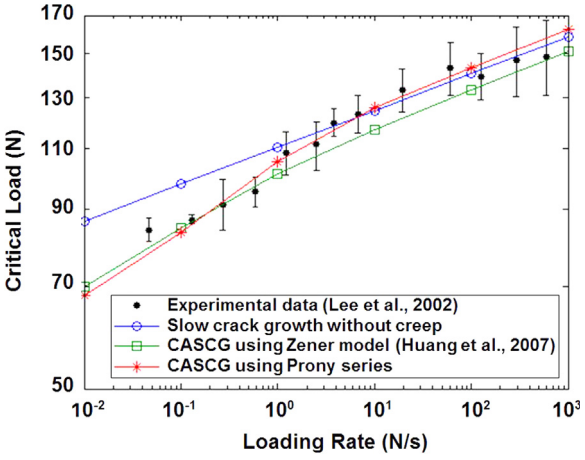

Fig. 7 – Critical "pop-in" loads obtained for glass-epoxy-polycarbonate multilayered structure under Hertzian contact loading at various loading rates. A comparison of experimental data (Lee et al., 2002) and predictions obtained using different materials models.

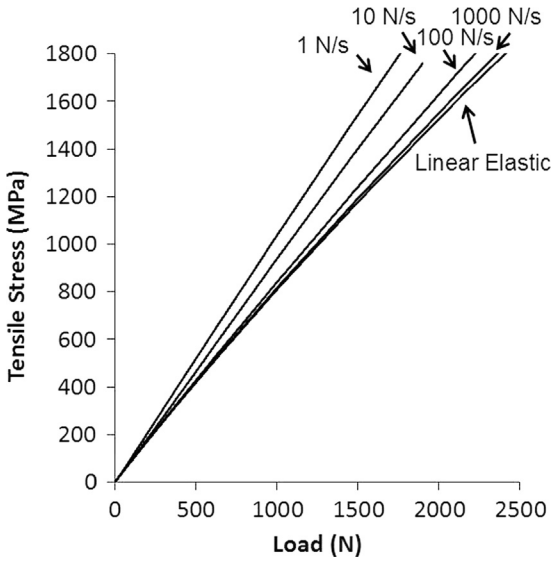

Fig. 8 – Computed tensile stresses in the sub-surface regions of the ceramic top layers. These were obtained as a function of Hertzian contact load at various loading rates using linear elastic and viscoelastic models.

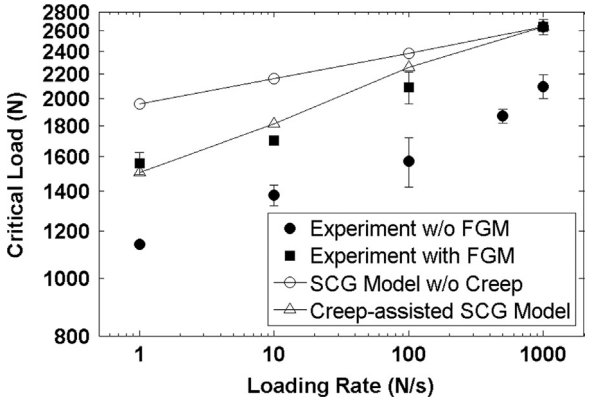

Fig. 9 – Rate-dependent critical loads of the zirconia-FGM-Z100 multilayers under Hertzian contact loading. A comparison of experimental data (Niu et al., 2009), prediction using SCG model without creep and prediction using CASCG model with Prony series.

The critical "pop-in" loads obtained for the FGM structures (under Hertzian contact loading) at different loading rates are presented in Fig. 9. The critical pop-in loads (Niu et al., 2008) increased with increasing loading rates. For any given loading rate, the critical loads obtained for the FGM structures were greater than those obtained for the conventional tri-layer structures with single adhesive layer. The differences were greater for slower loading rates than they were for faster loading rates. For any given loading rate, the critical loads obtained from the experiments on FGM structures were lower than those predicted using linear elastic models in this study. The results also show clearly that the predictions from the CASCG model were in closer agreement with the experimental results obtained from the FGM structures.

4.4. *Implications*

The current results suggest that the critical loads for failure in dental multilayers can be estimated accurately when the effects of viscosity in the polymeric substrate and adhesive layers are accounted for. This is especially true when the model captures the distribution of relaxation times for polymers due to the heterogeneity of the polymer. Furthermore, failure to model the viscosity of individual layers in dental multilayers may result in non-conservative predictions of "pop-in" loads or structural life. This is especially true in the high cycle fatigue regime where the effects of viscosity are likely to be more significant. Further studies of contact-induced failure are needed to explore the effects of cyclic loading and environments that are relevant to occlusal contact. There is, also, a need to study real teeth and actual crown geometries that incorporate the combined effects of slow crack growth in the top ceramic layers and viscosity of the adhesive and substrate layers. These are clearly some challenges for future work.

5. Conclusions

This paper presents the results of a combined experimental and analytical/computational study of the effects of creep

behavior on the contact-induced fracture of bio-inspired dental FGM structures and the conventional tri-layer structures. The creep effects in the adhesive layer and substrate layer play an important role in determining the critical "pop-in" loads at various loading rates under Hertzian contact. The loading rate effects on the critical loads of dental multilayers can be explained by a combination of the adhesive and substrate layer creep and the creep-assisted slow crack growth in the ceramic layer. The adhesive and substrate layer creep are well predicted by Prony series with three exponential terms.

Acknowledgments

This research was supported by the National Institute of Health (Grant no. P01DE10956), the National Science Foundation (Grant no. 0231418) and the Strategic Research Grant from the City University of Hong Kong (Grant No. 2011SRG067). The authors are grateful to the program managers, Dr. Eleni Kouslevari (NIH) and Dr. Carmen Huber (NSF), for their support. Appreciation is also extended to Professor George Scherer of Princeton University, and Professors Dianne Rekow and Van Thompson of King's College London for useful technical discussions.

REFERENCES

Bower, A.F., 2011. In: Applied Mechanics of Solids. CRC Press.

Dabbs, T.P., Lawn, B.R., Kelly, P.L., 1982. A dynamic fatigue study of soda–lime silicate and borosilicate glasses using small scale indentation flaws. Phys. Chem. Glass 23, 58–66.

Du, J., Niu, X., Rahbar, N., Soboyejo, W., 2013. Bio-inspired dental multilayers: effects of layer architecture on the contact-induced deformation. Acta Biomater. 9, 5273–5279, http://dx.doi.org/10.1016/j.actbio.2012.08.034.

Huang, M., Niu, X., Shrotriya, P., Thompson, V., Rekow, D., Soboyejo, W.O., 2005. Contact damage of dental multilayers: viscous deformation and fatigue mechanisms. J. Eng. Mater. Technol. 127, 33, http://dx.doi.org/10.1115/1.1836769.

Huang, M., Niu, X., Soboyejo, W.O., 2007a. Creep induced rate effects on radial cracks in multilayered structures. J. Mater. Sci. Mater. Med. 18, 65–69, http://dx.doi.org/10.1007/s10856-006-0663-z.

Huang, M., Wang, R., Thompson, V., Rekow, D., Soboyejo, W.O., 2007b. Bioinspired design of dental multilayers. J. Mater. Sci. Mater. Med. 18, 57–64, http://dx.doi.org/10.1007/s10856-006-0662-0.

Kelly, J.R., 1997. Ceramics in restorative and prosthetic dentistry. Annu. Rev. Mater. Sci. 27, 443–468, http://dx.doi.org/10.1146/annurev.matsci.27.1.443.

Lawn, B.R., Lee, K.S., Chai, H., Pajares, A., Kim, D.K., Wuttiphan, S., Peterson, I.M., Hu, X., 2000. Damage-resistant brittle coatings. Adv. Eng. Mater. 2, 745–748, http://dx.doi.org/10.1002/1527-2648(200011) (2:11<745::AID-ADEM745>3.0.CO;2-E).

Lawn, B.R., Pajares, A., Zhang, Y., Deng, Y., Polack, M.a, Lloyd, I.K., Rekow, E.D., Thompson, V.P., 2004. Materials design in the performance of all-ceramic crowns. Biomaterials 25, 2885–2892, http://dx.doi.org/10.1016/j.biomaterials.2003.09.050.

Lee, C.-S., Kim, D.K., Sanchez, J., Pedro, M., Antonia, P., Lawn, B.R., 2002. Rate effects in critical loads for radial cracking in ceramic coatings. J. Am. Ceram. Soc. 85, 2019–2024.

Malament, K.A., Socransky, S.S., 1999. Survival of Dicor glass–ceramic dental restorations over 14 years: Part I. Survival of Dicor complete coverage restorations and effect of internal surface acid etching, tooth position, gender, and age. J. Prosthet. Dent. 81, 23–32.

Marshall, G.W., Balooch, M., Gallagher, R.R., Gansky, S.A., Marshall, S.J., 2001. Mechanical properties of the dentinoenamel junction: AFM studies of nanohardness, elastic modulus, and fracture. J. Biomed. Mater. Res. 54, 87–95.

McCrum, N.G., Buckley, C.P., Bucknall, C.B., 1997. Principles of Polymer Engineering. Oxford University Press.

Niu, X., Rahbar, N., Farias, S., Soboyejo, W., 2009. Bio-inspired design of dental multilayers: experiments and model. J. Mech. Behav. Biomed. Mater. 2, 596–602, http://dx.doi.org/10.1016/j.jmbbm.2008.10.009.

Niu, X., Soboyejo, W., 2006. Effects of loading rate on the deformation and cracking of dental multilayers: experiments and models. J. Mater. Res. 21, 970–975, http://dx.doi.org/10.1557/jmr.2006.0114.

Niu, X., Yang, Y., Soboyejo, W., 2008. Contact deformation and cracking of zirconia/cement/foundation dental multilayers. Mater. Sci. Eng. A 485, 517–523, http://dx.doi.org/10.1016/j.msea.2007.09.014.

Rahbar, N., Soboyejo, W.O., 2011. Design of functionally graded dental multilayers. Fatigue Fract. Eng. Mater. Struct. 34, 887–897, http://dx.doi.org/10.1111/j.1460-2695.2011.01581.x.

Rekow, D., Thompson, V.P., 2007. Engineering long term clinical success of advanced ceramic prostheses. J. Mater. Sci. Mater. Med. 18, 47–56, http://dx.doi.org/10.1007/s10856-006-0661-1.

Shrotriya, P., Wang, R., Katsube, N., Seghi, R., Soboyejo, W.O., 2003. Contact damage in model dental multilayers: an investigation of the influence of indenter size. J. Mater. Sci. Mater. Med. 14, 17–26.

Wiederhorn, S.M., 1974. Subcritical crack growth in ceramics. In: Bradt, R.C., Hasselman, D.P.H., Lange, F.F. (Eds.), Fracture Mechanics of Ceramics. Volume 2. Microstructure, Materials, and Applications. Springer, US, pp. 613–646, http://dx.doi.org/10.1007/978-1-4615-7014-1_12.

Zhang, Y., Pajares, A., Lawn, B.R., 2004. Fatigue and damage tolerance of Y-TZP ceramics in layered biomechanical systems. J. Biomed. Mater. Res., B. Appl. Biomater. 71, 166–171, http://dx.doi.org/10.1002/jbm.b.30083.

Zhou, J., Huang, M., Niu, X., Soboyejo, W.O., 2007. Substrate creep on the fatigue life of a model dental multilayer structure. J. Biomed. Mater. Res., B. Appl. Biomater. 82, 374–382, http://dx.doi.org/10.1002/jbm.b.30742.